

© Copyright 2016 American Meteorological Society (AMS). Permission to use figures, tables, and brief excerpts from this work in scientific and educational works is hereby granted provided that the source is acknowledged. Any use of material in this work that is determined to be “fair use” under Section 107 of the U.S. Copyright Act September 2010 Page 2 or that satisfies the conditions specified in Section 108 of the U.S. Copyright Act (17 USC §108, as revised by P.L. 94-553) does not require the AMS’s permission. Republication, systematic reproduction, posting in electronic form, such as on a web site or in a searchable database, or other uses of this material, except as exempted by the above statement, requires written permission or a license from the AMS. Additional details are provided in the AMS Copyright Policy, available on the AMS Web site located at (<https://www.ametsoc.org/>) or from the AMS at 617-227-2425 or [copyrights@ametsoc.org](mailto:copyrights@ametsoc.org).

**TABLE 2.3. Computed trends ( $^{\circ}\text{C decade}^{-1}$ ) for radiosonde, satellite, and reanalysis data for the periods: 1958–95, 1979–95, 1995–2015, and 1979–2015. 1995 is chosen as an inflection point distinguishing the earlier downward trend from the near-neutral trend of recent years.**

| Global (82.5°N–82.5°S) TLS Temperature Anomaly Trends<br>(1981–2010 base period) |         |         |           |           |
|--|---------|---------|-----------|-----------|
| Dataset  | 1958–95 | 1979–95 | 1995–2015 | 1979–2015 |
| Radiosonde   |         |         |           |           |
| RAOBCORE   | -0.117  | -0.306  | 0.260     | -0.208    |
| RICH   | -0.282  | -0.484  | 0.219     | -0.278    |
| RATPAC   | -0.257  | -0.649  | -0.010    | -0.467    |
| UNSW   | -0.330  | -0.474  | 0.039     | -0.317    |
| Satellite  |         |         |           |           |
| RSS  | ×       | -0.336  | -0.012    | -0.261    |
| STAR   | ×       | -0.364  | -0.002    | -0.262    |
| UAH  | ×       | -0.399  | -0.046    | -0.312    |
| Reanalysis   |         |         |           |           |
| CFSR   | ×       | -0.652  | 0.106     | -0.348    |
| ERA-Interim  | ×       | -0.187  | 0.199     | -0.119    |
| JRA-55   | ×       | -0.235  | 0.018     | -0.217    |
| MERRA-2  | ×       | -0.300  | 0.171     | -0.199    |

- 4) LAKE SURFACE TEMPERATURES—R. I. Woolway, K. Cinque, E. de Eyto, C. L. DeGasperi, M. T. Dokulil, J. Korhonen, S. C. Maberly, W. Marszelewski, L. May, C. J. Merchant, A. M. Paterson, M. Riffler, A. Rimmer, J. A. Rusak, S. G. Schladow, M. Schmid, K. Teubner, P. Verburg, B. Vigneswaran, S. Watanabe, and G. A. Weyhenmeyer

Lake summer surface water temperatures (LSSWT) in 2015 strongly reflected the decadal patterns of warming noted in the scientific literature. Northern Hemisphere summer refers to July–September whereas Southern Hemisphere summer refers to January–March. A recent worldwide synthesis of lake temperatures (O’Reilly et al. 2015) found that LSSWTs rose by, on average,  $0.034^{\circ}\text{C yr}^{-1}$  between 1985 and 2009, ~1.4 times that of the global surface air temperature (SAT) in general. Data from lakes in various regions collated here show that during 2009–15 lake temperatures continued to rise.

During 2015, LSSWT of many lakes exceeded their 1991–2010 averages by  $1^{\circ}\text{C}$  or more (Online Fig. S2.6; Plate 2.1c). Strong warm anomalies in LSSWT were most prominent in central Europe [Austria, Switzerland, and Poland (data from the Institute of Meteorology and Water Management, Poland)], where anomalies above  $1^{\circ}\text{C}$  were recorded. The hot central European summer (JJA) of 2015 (sections 2b6 7f, and Sidebar 7.1) is reflected in relatively high

mean LSSWTs in three Austrian lakes (Mondsee, Neusiedler See, Wörthersee; Fig. 2.6; Online Fig. 2.6) with anomalies up to  $+1.6^{\circ}\text{C}$ . Similarly, satellite-based LSSWT anomalies of 25 European lakes in and near the Alps were in excess of  $1.0^{\circ}\text{C}$  in 2015 (Fig. 2.7a), the second warmest anomaly year since the record summer of 2003 (Beniston 2004). High LSSWTs were also observed in other regions of the world (Plate 2.1c; Online Fig. 2.6), with anomalies for lakes in Seattle [Washington (state), U.S.], for example, up to  $+1^{\circ}\text{C}$  in 2015.

LSSWTs are influenced by a combination of broad climatic vari-

ability and local characteristics, so regional and subregional differences in LSSWTs are common. LSSWTs in Britain and Ireland during 2015 were  $\sim 0.6^{\circ}\text{C}$  below average, in contrast to central Europe. This likely reflects cool anomalies in SAT in early and mid-2015 (e.g., [www.met.ie/climate/MonthlyWeather/clim-2015-ann.pdf](http://www.met.ie/climate/MonthlyWeather/clim-2015-ann.pdf)).

Although the Great Lakes (United States and Canada) have warmed faster than SAT in recent decades, the 2015 LSSWTs were relatively cool. This is attributable to above-average winter ice cover during 2014/15, which shortened the warming season. The annual maxima of percent ice cover (Great Lakes Environmental Research Laboratory; [www.glerl.noaa.gov/](http://www.glerl.noaa.gov/)) in 2014 (92.5%) and 2015 (88.8%) were substantially above the 1973–2015 average (53.2%). These were the first consecutive high-ice-cover years since the 94.7% maximum ice coverage recorded in 1979. The strong El Niño conditions of 2015 lessen the chance that 2016 will imitate 2014 and 2015.

Despite these recent cooler LSSWTs, the average warming rate for the Great Lakes is approximately  $0.05^{\circ}\text{C yr}^{-1}$  (1979–2015). This rate contrasts with the Dorset lakes in Ontario, Canada (surface areas  $<100$  ha), which do not show a statistically significant trend in LSSWT between 1980 and 2015. In 2015, LSSWT anomalies in these lakes were  $\sim +0.6^{\circ}\text{C}$ . These

lakes display large interannual variation in LSSWT, mainly reflecting interannual differences in SAT, with strong agreement in high and low years.

The relationship between SAT and LSSWT can be complicated by several processes. For Lake Erken, Sweden, LSSWT is strongly influenced by water col-

umn mixing and precipitation, leading to a relatively weak relationship between SAT and LSSWT. The LSSWT of New Zealand's largest lake, Lake Taupo, is thought to be influenced by interannual variation in geothermal heating (de Ronde et al. 2002) and shows no significant trend. Furthermore, an analysis of the 47-year record (1969–2015) of LSSWT from Lake Kinneret, Israel, reveals warming of  $\sim 1.65^\circ\text{C}$  over the period ( $\sim 0.036^\circ\text{C yr}^{-1}$ ). Two factors explain most of the variability ( $r^2 = 0.67$ ): SAT and water levels (Rimmer et al. 2011; Ostrovsky et al. 2013).

In recent years there has been a strong emphasis on investigating LSSWT warming, with only a few investigations focusing on the winter months (e.g., Dokulil et al. 2014) due to a lack of available data. Winter temperature changes can be quite distinct from LSSWT trends. For example, the regional average warming rate for lakes in Britain and Ireland is substantially higher during winter ( $0.028^\circ\text{C yr}^{-1}$ ; Fig. 2.7b) than in summer ( $0.018^\circ\text{C yr}^{-1}$ ; Fig. 2.7d). Future assessments that focus on all seasons will provide a more complete picture.

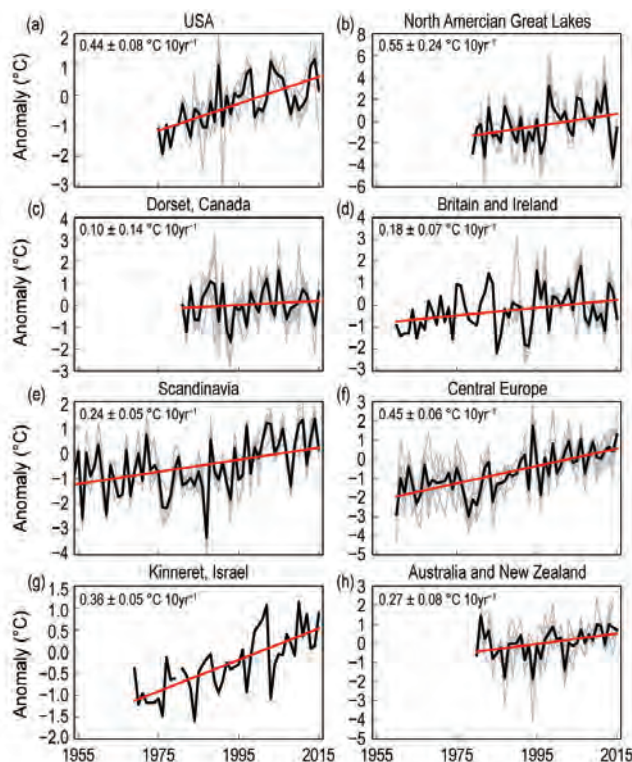


**FIG. 2.6.** Lake summer (Jul–Sep in Northern Hemisphere, Jan–Mar in Southern Hemisphere) surface water temperature anomalies relative to 1991–2010 for (a) the United States (Washington, Sammamish, Union, and Tahoe); (b) the Laurentian Great Lakes, [Superior (buoys 45001, 45004, 45006), Michigan (buoys 45002, 45007), Huron (buoys 45003, 45008), and Erie (buoy 45005)]; (c) Dorset, Ontario, Canada [Blue Chalk, Chub, Crosson, Dickie, Harp, Heney Plastic, and Red Chalk (East and Main basin)]; (d) Britain and Ireland [Bassenthwaite Lake, Blenheim Tarn, Derwent Water, Esthwaite Water, Lough Feeagh, Grasmere, Loch Leven, and Windermere (North and South basins)]; (e) Scandinavia (Erken, Inarijärvi, Kitisjärvi, Lappajärvi, Päijänne, Pielinen, and Saimaa); (f) central Europe (Charzykowskie, Jeziorak, Lubie, Mondsee, Neusiedler See, Wörthersee, and Zurich); (g) Israel (Kinneret); and (h) Australia and New Zealand (Burragorang, Cardinia, Sugarloaf, Taupo, and Upper Yarra). Gray lines indicate the temperature for each individual lake and the thick black line indicates the average lake temperature for the specified region. The trend for the regionally averaged temperatures is shown in red, and the equation describing the change is presented. Note that the warming rates are not comparable among the different regions due to the different time periods shown.

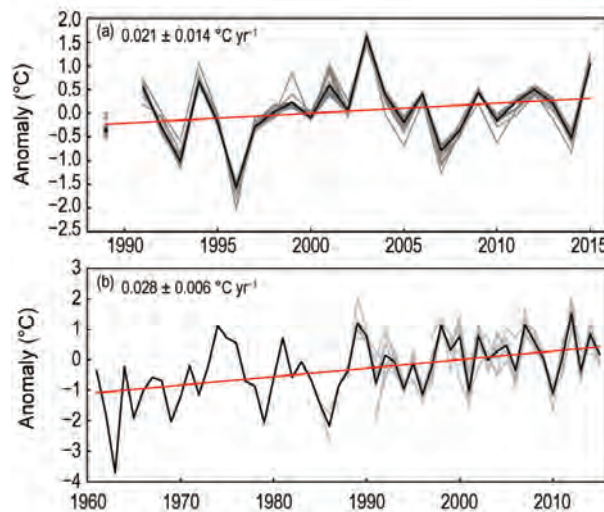


**FIG. 2.7.** Satellite-derived lake surface water temperature anomalies for (a) summer (Jul–Sep; 1991–2015) for European Alpine lakes (all natural water bodies in or near the Alps larger than  $14 \text{ km}^2$ ; Riffler et al. 2015) and (b) winter (Jan–Mar, 1961–2015) for Britain and Ireland (base period: 1991–2010). Gray lines indicate the temperature for each individual lake and the thick black line indicates the average lake temperature for the region. The trend for the regionally averaged temperatures is shown in red, and the equation describing the change is presented. The lakes included are the same as those shown in Online Fig. 2.6 and Plate 2.1c.